International Journal of Biological Macromolecules 273 (2024) 133187

Contents lists available at ScienceDirect

International Journal of Biological Macromolecules

journal homepage: www.elsevier.com/locate/ijbiomac

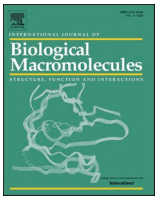

# PCNA molecular recognition of different PIP motifs: Role of Tyr211 phosphorylation

Antonio Ruiz-Albor [a], Belén Chaves-Arquero [a], Inés Martín-Barros [b], Alejandra Guerra-Castellano [c], Amaia Gonzalez-Magaña [d], Alain Ibáñez de Opakua [b], Nekane Merino [b], Mariola Ferreras-Gutiérrez [a], Edurne Berra [b], Irene Díaz-Moreno [c], Francisco J. Blanco [a,*]

[a] Centro de Investigaciones Biológicas Margarita Salas (CIB), CSIC, Madrid 28040, Spain
[b] CIC bioGUNE, Derio 48160, Spain
[c] Instituto de Investigaciones Químicas, cicCartuja, Universidad de Sevilla-CSIC, Sevilla, Spain
[d] Instituto Biofisika, CSIC-UPV/EHU, 48940 Leioa, Spain.

ARTICLE INFO

*Keywords:*
PCNA
Molecular recognition
DNA replication

ABSTRACT

The coordination of enzymes and regulatory proteins for eukaryotic DNA replication and repair is largely achieved by Proliferating Cell Nuclear Antigen (PCNA), a toroidal homotrimeric protein that embraces the DNA duplex. Many proteins bind PCNA through a conserved sequence known as the PCNA interacting protein motif (PIP). PCNA is further regulated by different post-translational modifications. Phosphorylation at residue Y211 facilitates unlocking stalled replication forks to bypass DNA damage repair processes but increasing nucleotide misincorporation. We explore here how phosphorylation at Y211 affects PCNA recognition of the canonical PIP sequences of the regulatory proteins p21 and p15, which bind with nM and μM affinity, respectively. For that purpose, we have prepared PCNA with *p*-carboxymethyl-*L*-phenylalanine (pCMF, a mimetic of phosphorylated tyrosine) at position 211. We have also characterized PCNA binding to the non-canonical PIP sequence of the catalytic subunit of DNA polymerase δ (p125), and to the canonical PIP sequence of the enzyme ubiquitin specific peptidase 29 (USP29) which deubiquitinates PCNA. Our results show that Tyr211 phosphorylation has little effect on the molecular recognition of p21 and p15, and that the PIP sequences of p125 and USP29 bind to the same site on PCNA as other PIP sequences, but with very low affinity.

## 1. Introduction

Murine embryos die early when the Proliferating Cell Nuclear Antigen (PCNA) gene is knocked down [1], consistent with the high importance of the PCNA protein in the replication of DNA [2]. PCNA has a ring-shape structure embracing the DNA duplex, and interacts with many other proteins that modify the DNA molecule or regulate DNA-related processes [3]. These interactions occur frequently through short linear sequence motifs in disordered regions of the PCNA partners [4]. The PCNA interacting protein motif (PIP) is the best characterized one, with the consensus sequence *QXXhXXaa*, where *h* is a hydrophobic aliphatic residue (frequently Met, Leu or Ile), *a* is an aromatic residue (frequently Phe or Tyr), and *X* is any residue. However, sequence diversity is large and it has been proposed that the PIP is not a distinct motif but part of a loosely defined set of PIP-like motifs with overlapping specificities for several proteins involved in genome maintenance [5]. This set includes the PIP, the APIM (AlkB homolog 2 PCNA-interacting motif), the RIR (Rev1-interacting region), the MIP (Mlh1-interacting protein), and the F1 motifs. The major structural feature of PIP-like motifs bound to its partners is two or three apolar residues inserted into hydrophobic pockets. When bound to PCNA, these residues form a short helix on the PCNA protomer. The archetypal complex structure is that of the PIP of cell-cycle checkpoint protein $p21^{WAF1/CIP1}$ (hereafter named p21) [6]. The co-crystal shows that residues located C-terminally to the PIP ones also interact with PCNA, contributing to the high affinity of the interaction of p21 with PCNA, in the nM range. With some differences, all experimentally determined structures of PIP-like motifs bind to the same site on each of the three PCNA protomers, at the front

* Corresponding author.
*E-mail address:* fj.blanco@cib.csic.es (F.J. Blanco).

https://doi.org/10.1016/j.ijbiomac.2024.133187
Received 6 May 2024; Received in revised form 11 June 2024; Accepted 13 June 2024
Available online 14 June 2024

face of the PCNA ring (the one oriented towards DNA synthesis progression). The major difference is observed for the PCNA associated factor p15 (hereafter p15), of which residues N-terminally to the PIP ones interact with the inner side of the PCNA ring [7] threading the protein through it [8], although the overall affinity is lower than for p21, in the μM range.

The replication of the DNA lagging strand in human cells proceeds discontinuously by elongation of short primers (synthesized by polymerase α) into Okazaki fragments that are later ligated [9]. Elongation is done by DNA polymerase δ (hereafter Pol δ), whose processivity and rate of nucleotide incorporation are increased when anchored to PCNA. Pol δ consists of the catalytic subunit p125, harboring the polymerase and exonuclease activities, and regulatory subunits p50, p66 (also known as p68), and p12. It has been reported that the four subunits are able to directly bind to PCNA. The PIP of p66 and the PIP-like motifs of p12 bind to the same site on PCNA with micromolar affinity, as seen in their crystal structures [10,11]. The catalytic subunit p125 binds to PCNA with nM affinity mediated by a PIP-like motif as seen by mutagenesis experiments [12], while p50 binding to PCNA is unclear or occurs with very low affinity [13]. However, in the cryogenic electron microscopy (cryo-EM) structure of the replication-competent holoenzyme (Pol δ-PCNA-DNA) only p125 is bound to PCNA [14]. The motifs of p66 and p12 are located in regions predicted as disordered that are not visible in the micrographs. A PIP-like motif of p125 occupies the corresponding binding site on one of the PCNA protomers, the other two remaining free of bound ligand. Another PIP-like motif of p125 interacts with the p50

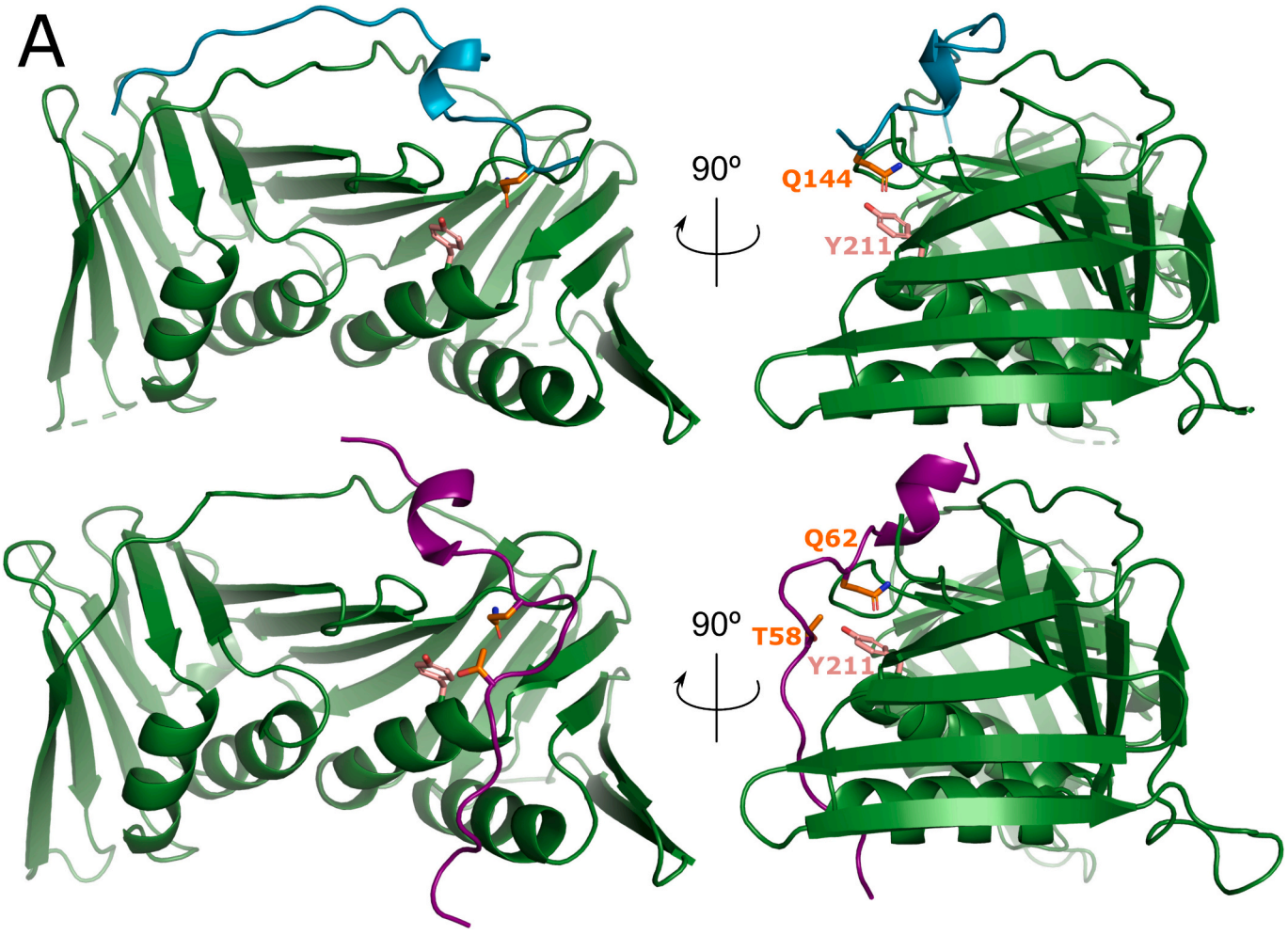


B

| | | |
|---|---|---|
| p21 | (139-160) | GRKRRQTSMTDFYHSKRRLIFS |
| p15 | (50-77) | GNPVCVRPTPKWQKGIGEFFRLSPKDSE |
| p125 | (996-1009) | yrrgTGKVGGLLAFAKRR |
| USP29 | (458-485) | LHQETKPLPLSIQNSLDLFFKEEELEYN |

**Fig. 1.** (A) Ribbon diagrams of the crystal structure of PCNA (green) bound to the p21 (cyan) or the p15 (purple) PIP fragments (Protein Data Bank entries are 1ACX and 4D2G, respectively). For simplicity only one of the three protomers of the PCNA homotrimer, and the corresponding bound p21 or p15 fragment, is shown. The side chains of Tyr211 in PCNA, Q144 in p21, and Gln62 and Thr58 in p15 are shown in sticks, with carbons colored wheat (Tyr211) or orange. (B) Amino acid sequence of the protein fragments of which binding to PCNA is studied. The residues matching the canonical PIP motif are highlighted in bold, and those colored in orange correspond to the side chains in sticks in panel A. Lower case letters in p125 indicate non-native residues added to facilitate solubility and concentration measurement. (For interpretation of the references to colour in this figure legend, the reader is referred to the web version of this article.)

subunit, and not with PCNA. Consistent with this structure, mutation of the p125 motif bound to PCNA has a larger deleterious impact on DNA primer extension than mutation of the p12 or p66 ones [14]. The structure of the *S. cerevisiae* complex shows the corresponding PIP-like motif of Pol3 subunit (the homolog of human p125) bound to one protomer of the PCNA ring [15], and mutations in this motif reduce the PCNA-stimulated activity of Pol3 [16].

Different post-translational modifications (PTM) have been detected in human PCNA, and for some of them the effect on DNA-related biological processes has been investigated. When DNA damage stalls the replication fork PCNA is monoubiquitinated at Lys164 facilitating error-prone translesion DNA synthesis (TLS), or polyubiquitinated facilitating the error-free template switching mechanism of DNA damage tolerance [17]. PCNA can be deubiquitinated by several ubiquitin specific peptidases, among them USP29 [18], a promiscuous deubiquitinase that contains a PIP motif. PCNA is phosphorylated at Tyr211 by the epidermal growth factor receptor [19] stabilizing the DNA replication fork, against stalling or collapse, at the expense of increased nucleotide misincorporation [20]. High levels of PCNA with phosphorylated Y211 in human primary breast tumor tissues correlate with poor survival [21]. In the structure of PCNA, Tyr211 is solvent exposed, and its phosphorylation is not expected to modify the structure or stability of the PCNA ring, however, it is located close to the PIP binding site on the front face of the ring and could affect its molecular recognition properties (Fig. 1). The side chain of Tyr211 in PCNA is close to the glutamine residues in the PIP motifs of p21 and p15 and is also close to the side chain of Thr58 in p15 as seen in the crystal structures of the complexes (Fig. 1). Adding the phosphoryl group to the oxygen of Tyr211 might destabilize the PCNA interaction with both proteins because of the increased size and negative charge. To test this hypothesis, we have prepared PCNA Y211-pCMF, a mimetic of PCNA phosphorylated at Tyr211 by incorporating the non-natural amino acid pCMF [22]. We have used isothermal titration calorimetry (ITC) to measure the effect of the mimetic on PCNA affinity for the regulatory proteins p21 and p15 and found a very small effect. We have also used NMR to measure the binding of PCNA to the PIP of USP29 and to the PIP-like of p125, finding that they bind to the same site on the PCNA protomer but with low affinity.

## 2. Results

### 2.1. The PIP-like motif of p125 binds to PCNA with micromolar affinity

The binding of the PIP-like motif of p125 was observed by solution NMR on an isotopically enriched PCNA sample titrated with p125 peptide (Fig. 2A, and B). Many $^{1}H$-$^{15}N$ correlation NMR signals from PCNA experienced gradual chemical shift perturbations (CSP) indicating that the peptide binds to the three protomers with a fast exchange kinetics (with respect to the difference in chemical shifts between the free and bound forms). The pattern of CSP along the PCNA sequence and its mapping on the PCNA structure (Fig. 2C, and D) shows that p125 binds to each protomer of PCNA on the hydrophobic patch lined by the C-terminal residues, the interdomain connecting loop (IDCL), and loops of the central β-sheet. This is similar to p21 binding, but the large molar excess of peptide necessary for saturation indicates much lower affinity. The titration of the signals from residues with CSP values larger than the average plus two standard deviations yielded a dissociation constant of 91 ± 7 μM at 35 °C (Fig. 2B). Attempts to obtain well-diffracting crystals for structure determination of the complex were unsuccessful.

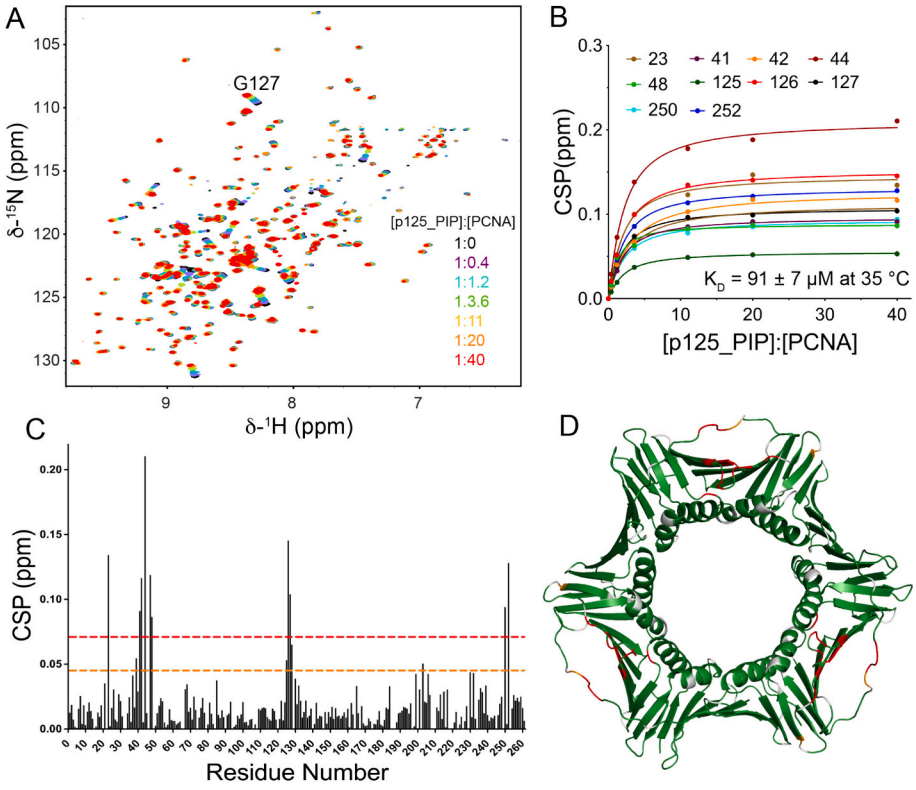


**Fig. 2.** (A) Superposition of $^{1}H$-$^{15}N$ TROSY spectra of 60 μM PCNA in the presence of p125 peptide at increasing molar ratios (from black to red). The signal of Gly27 is labeled to illustrate signal shifting. (B) Chemical shift perturbation (CSP) of backbone amide NMR signals of PCNA at increasing molar ratios. The symbols correspond to the experimental data and the continuous line to the best fit to a model of one set of identical binding sites. Only residues with a CSP larger than the average plus two standard deviations are shown, and were used to calculate the average dissociation constant. (C) CSP caused by p125 peptide along the PCNA residue number. The orange and red dashed lines indicate the average plus one or two standard deviations, respectively. (D) Mapping of the residues with CSP smaller than the average (green), larger than the average plus one (orange) or two (red) standard deviations, or with no measured CSP (grey). (For interpretation of the references to colour in this figure legend, the reader is referred to the web version of this article.)

### 2.2. The PIP motif of USP29 binds to PCNA with millimolar affinity

The binding of the PIP motif of USP29 was examined by solution NMR in a similar way as p125, however, changes much smaller than those for the p125 peptide at similarly high molar excess were observed (Fig. 3A, and B), indicating very weak binding. Still, the pattern of CSP along the PCNA sequence and its mapping on the PCNA structure (Fig. 3C, and D) shows that the peptide binds to the same region as p125 and other PIP or PIP-like motifs. The titration of the signal from G127 yields an estimated dissociation constant of 3 ± 1 mM at 35 °C (Fig. 3E). Attempts to prepare samples of the full-length USP29 protein were unsuccessful because the protein was insoluble in bacterial cells and its production levels were very low in mammalian cells.

### 2.3. PCNA phosphorylation at Tyr211 has little effect on the binding of p21 and p15 PIP motifs

PCNA incorporating *p*CMF at position 211 was produced with low yield but pure enough to confirm its nature and structural integrity (Fig. 4). Mass spectrometry of tryptic fragments showed the unique peptide with sequence YLNFFTK, corresponding to PCNA residues 211–217, with a mass 42 Da larger in PCNA Y211-pCMF than in PCNA (Fig. 4B). Peptide-spectrum match scores indicate that 98 % of the detected peptide molecules show this mass increase, while it was less than 5 % for other tryptic fragments containing tyrosine residues. Size Exclusion Chromatography with multiangle light scattering detection (SEC-MALS) showed that PCNA Y211-pCMF is a stable homotrimer in solution, with a measured molar mass of 87.2 kDa (the calculated one is 87.3 kDa).

The effect of pCMF incorporation at position 211 of PCNA on the

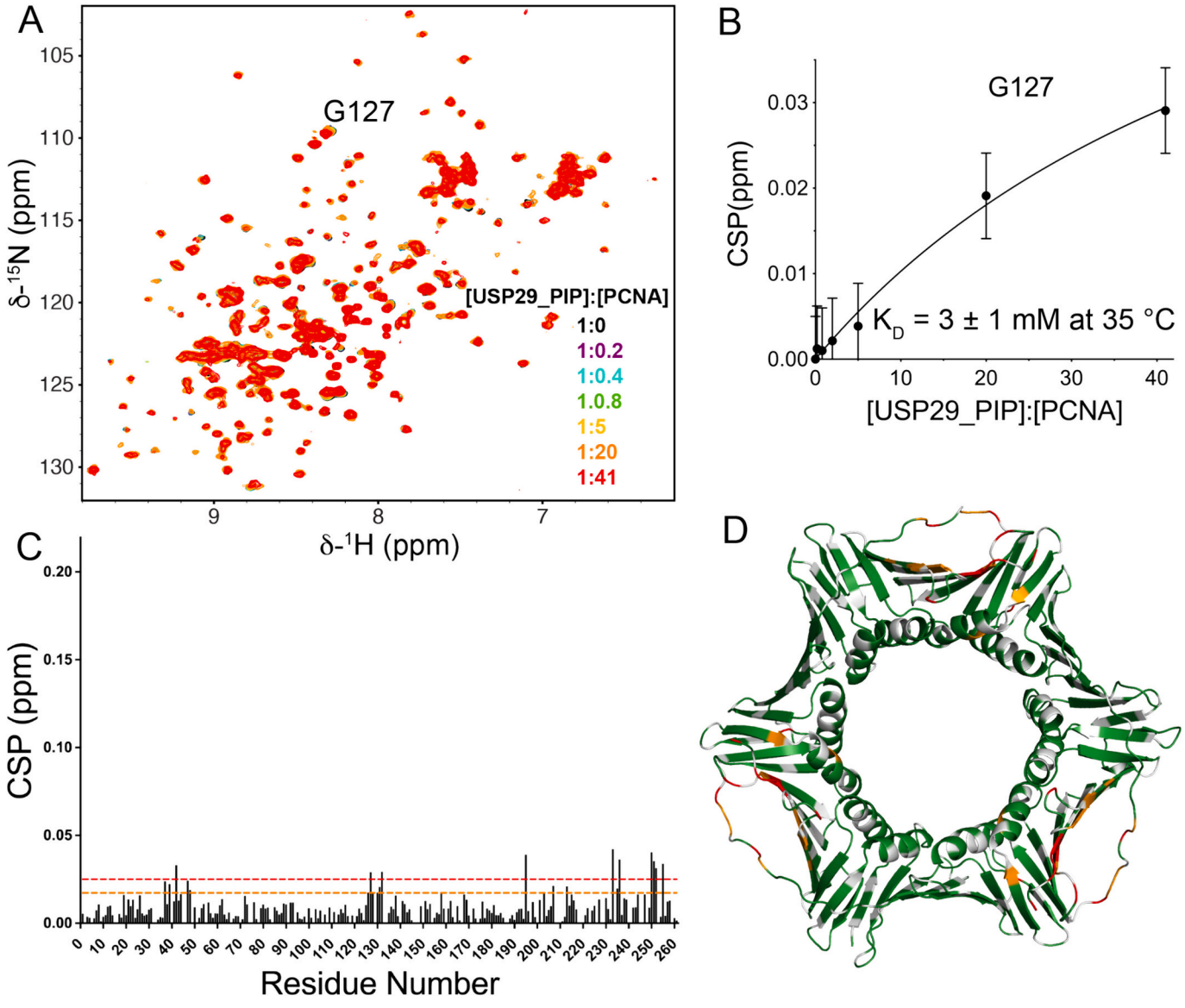


**Fig. 3.** (A) Superposition of $^{1}H$-$^{15}N$ HMQC spectra of 50 μM in the presence of USP29 peptide at increasing molar ratios (from black to red). (B) Chemical shift perturbation (CSP) of Gly127 amide NMR signal of PCNA at increasing molar ratios. The symbols correspond to the experimental data, the bar the estimated error, and the continuous line the best fit to a model of one set of identical binding sites. Other residues yielded very bad fittings. The error bar (±0.005 ppm) indicates the estimated error. (C) CSP caused by USP29 peptide along the PCNA residue number. The orange and red and dashed lines indicate the average plus one or two standard deviations, respectively. (D) Mapping of the residues with CSP smaller than the average (green), larger than the average plus one (orange) or two (red) standard deviations, or with no measured CSP (grey). (For interpretation of the references to colour in this figure legend, the reader is referred to the web version of this article.)

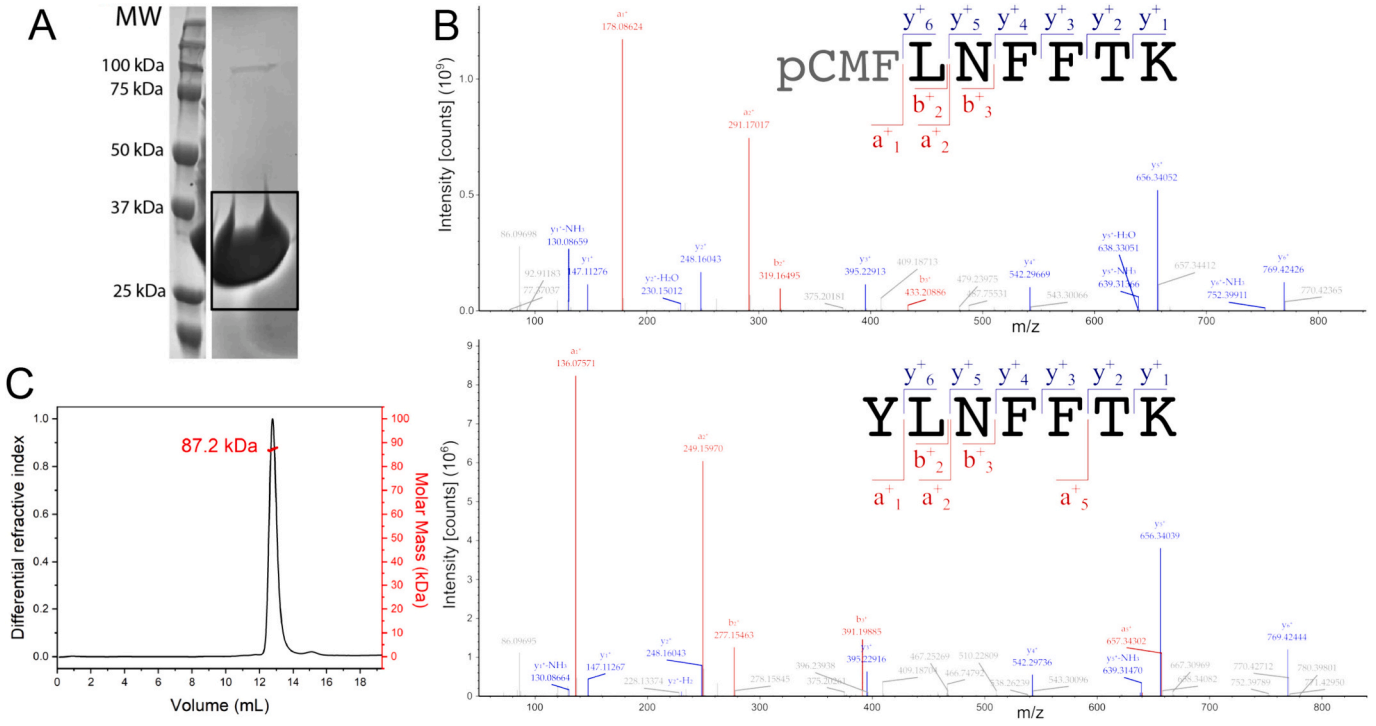


**Fig. 4.** (A) Reducing SDS-PAGE (12 % acrylamide) analysis of the purified PCNA Y211-pCMF. The left lane shows the molecular weight markers, the right lane the protein, and the square the band analyzed by mass spectrometry. (B) Identification of the pCMF incorporation at position 211 by liquid chromatography electrospray ionization tandem mass spectrometry (LC/ESI-MS/MS) of the tryptic fragment corresponding to residues 211–217. The spectrum corresponding to the chromatogram peak of PCNA with $m/z = 932.4885$ is shown at the bottom, and the spectrum corresponding to the chromatogram peak of PCNA Y211-pCMF with $m/z = 974.4980$ is shown at the top. The major ions identifying the peptide sequence are labeled, colored by mass series, and indicated in the scheme of peptide fragmentation inside each panel. (C) SEC-MALS of PCNA Y211-pCMF. The black line corresponds to the differential refractive index (left axis) and the red line to the measured molar mass (right axis). (For interpretation of the references to colour in this figure legend, the reader is referred to the web version of this article.)

interactions with the PIP motifs of p21 and p15 was evaluated by measuring the affinity by ITC at 35 °C. As seen in Fig. 5, a small increase in the affinity for p21 is observed, while no significant change occurs with p15.

## 3. Discussion

The dissociation constant of human Pol δ for a primer/template DNA junction (P/T) is approximately 540 nM, and is smaller than 10 nM when the DNA is bound to PCNA, as measured by fluorescence polarization in solution [23]. The two orders of magnitude increase in affinity must be due to PCNA interacting with the p125 subunit, the only one bound to PCNA in the cryo-EM structure of the complex [14]. Our results show that the PIP-like motif of p125 binds to the same region on the PCNA protomer as seen in the structure of the holoenzyme, where it binds as a one-turn helix [14]. However, the dissociation constant is 91 μM at 35 °C, indicating that the PIP-like sequence contributes but does not account for the overall nM affinity. This is consistent with the cryo-EM structure showing another sequence of p125 adjacent to the PIP-like one interacting as an antiparallel β-strand with the IDCL of the same PCNA protomer. Other authors have reported that the isolated p125 binds to immobilized PCNA with a $K_D$ of 100 nM at 20 °C, and that mutation of three residues of the PIP-like motif to alanine abrogates the binding [12]. These inconsistent results might be due to the different experimental design, the use of GST-fusion proteins and protein immobilization for surface plasmon resonance measurements. Analogously to the structure of the Pol δ holoenzyme, the structures of DNA polymerase κ [24] or DNA ligase 1 [25] holoenzymes showed that only one of the enzyme PIP-like motifs are bound to one of the PCNA protomers, with two protomers remaining unoccupied. These observations led the authors to propose a functional hierarchy of the PCNA interacting motifs: while motifs close to the catalytic core (proximal motifs) are necessary to anchor the enzyme to the PCNA ring, other motifs (distal motifs, frequently present in disordered terminal regions), are ancillary ones, possibly accelerating the initial recruitment of the enzyme to the DNA substrate before the proximal one binds and the complex is stabilized by other interactions [26]. The distal motifs might also act as flexible tethers when the enzymes occasionally fall off the DNA, and Pol δ is found to be only loosely bound to PCNA while synthesizing new DNA [23]. It was also hypothesized that the reason why distal motifs are canonical PIP ones is to confer high affinity, while proximal motifs are PIP-like to confer conformational diversity. However, our results show that some canonical PIP motifs bind with very low affinity.

The canonical PIP-motif of USP29 binds PCNA with an extremely low affinity, questioning its physiological relevance. We have reported that the canonical PIP motif of RecQ5 helicase (**Q**NLIRH**FF**) binds PCNA with low affinity ($K_D$ = 210 ± 50 μM at 35 °C) [11], but the PIP motif of USP29 binds PCNA with an even much lower affinity. This unexpected result shows that we still do not understand relevant aspects of the molecular recognition of PCNA by this class of short linear sequence motifs. It also shows the limitations in the use of short peptides to characterize the molecular recognition between proteins. The structure of USP29 is not known, but sequence analysis indicates that it has a split catalytic domain [27]. The AlphaFold model suggests that the PIP sequence is folded as a two-turn helix as part of the catalytic domain but far away from the active site. If the Alphafold model is correct, the structure of the PIP sequence would not be compatible with the canonical structure of PIP motifs bound to PCNA. However, the possibility of the isolated PIP sequence having a strong conformational preference interfering with PCNA binding can be ruled out because the $^1$H NMR signals of the peptide are non-dispersed, with chemical shift close to random coil values (data not shown). Further experiments will be

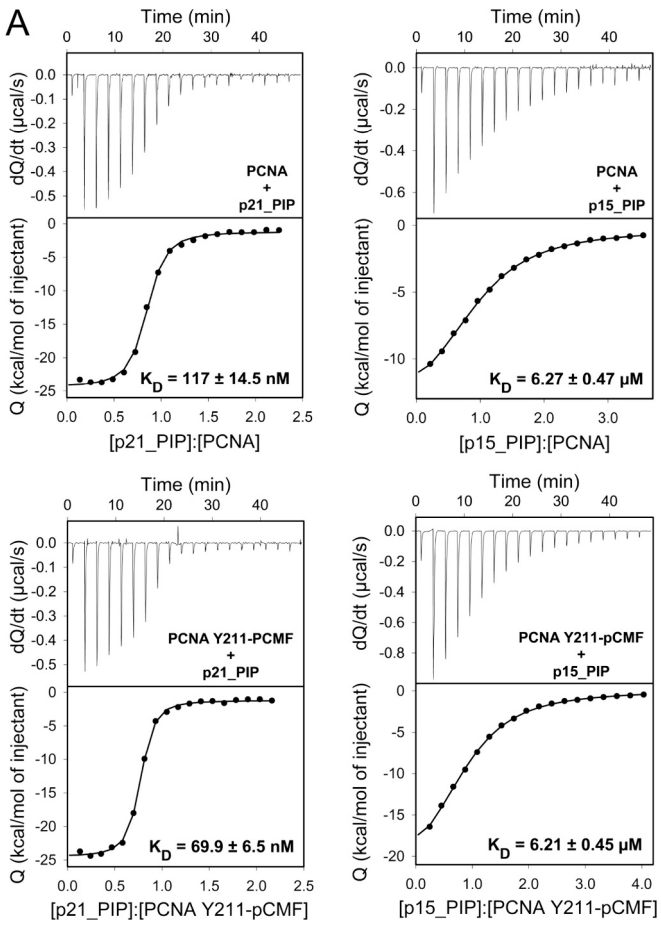


**Fig. 5.** Isothermal calorimetric titration of PCNA proteins with the PIP sequences of p21 (A) and p15 (B). The upper panels show the change of heat with time after the injections of peptide solution, and the lower panels the dependence of the heat released upon binding, after correction for the heat of dilution, with the molar ratio. The circles correspond to the experimental data and the continuous line to the best fit to a model of one set of identical binding sites.

necessary to understand how USP29 interacts with PCNA, but a complete structural analysis is hampered by the low solubility of the 922-residue long USP29 protein.

PCNA regulation by PTMs is still poorly understood. The most studied PTM is monoubiquitination at Lys164, which is important (though not essential) for TLS in mammalian cells [28]. TLS involves replacing stalled replicative polymerases by TLS polymerases, which have ubiquitin binding domains. It has been assumed that monoubiquitination of PCNA serves to recruit TLS polymerases, but biochemical experiments show that TLS is independent of PCNA monoubiquitination, suggesting an indirect role of this PTM in TLS enhancement [29]. USP29 contains two ubiquitin interacting motifs, likely binding ubiquitinated PCNA with higher affinity than non-ubiquitinated PCNA. Acetylation of lysine residues at the inner side of the PCNA ring, the sliding surface on the DNA, have been reported to regulate DNA repair [30,31]. Phosphorylation of PCNA at Tyr211 by epidermal growth factor receptor is linked to replication fork stabilization, but at high levels correlates with malign cancer. The structural basis of this effect remains unknown. The hypothesis that Tyr211 phosphorylation could interfere with the recognition of two regulators with high affinity for PCNA (p21 and p15) is not confirmed by our experiments with the isolated proteins. The affinity of PCNA for the PIP-like motifs of p125 or the PIP motif of USP29 is low and could not be measured by calorimetry, but considering the small effect of the mimetic of Tyr211 phosphorylation on p21 and p15 binding, it is likely to be of little consequence as well. In the context of the chromatin, with PCNA loaded on the DNA and bound to the full-length proteins, the effect might be more significant. Alternatively, there may be a yet unidentified protein that recognizes this PCNA modification and exerts the observed effect stabilizing the DNA replication fork.

## 4. Experimental procedures

### 4.1. Protein production and purification

The open reading frame (ORF) coding for human PCNA (UniProt: P12004) was cloned in a modified pET28 plasmid, including an N-terminal $His_6$-tag followed by a HRV 3C protease cleavage site. An analogous synthetic ORF was designed with an amber stop codon at Tyr211 to incorporate the non-natural amino acid pCMF and an ochre codon to terminate translation. This open reading frame, with codons optimized for production in *E. coli*, was purchased from Genscript cloned in plasmid pET29a(+). PCNA was produced in transformed *E. coli* BL21 (DE3) Rosetta cells grown in LB medium with antibiotics kanamycin (at 30 mg/l, for the pET28 plasmid with the PCNA ORF) and chloramphenicol (at 20 mg/l, for the pLysS plasmid in the Rosetta cells, producing the tRNAs that are common in human ORFs but rare in *E. coli* and the T7 lysozyme ORF). PCNA production was induced with 1 mM IPTG at 20 °C for about 20 h. PCNA with pCMF at residue 211 was produced in *E. coli* BL21(DE3) cells transformed with both the PCNA plasmid and the pEVOL plasmid grown in minimal medium M9 with the same antibiotics (kanamycin for the plasmid with the mutant PCNA ORF and chloramphenicol for the pEVOL plasmid). The pEVOL plasmid codes for the *M. jannaschii* aminoacyl-tRNA synthetase/suppressor tRNA pair specific for the pCMF amino acid [32], and the protein production protocol is similar to the previously described for cytochrome *c* [33]. A single colony of freshly transformed cells was used to inoculate a 125 ml culture in LB medium which was grown for approximately 15 h at 37 °C. A volume of 25 ml from the saturated culture was used to inoculate a 250 ml of LB culture grown at 37 °C until an optical density (OD) of 0.4 at 600 nm. At that moment, production of the tRNA and aminoacyl-tRNA synthetase pair was induced with 0.02 % arabinose. After 2 h, 200 ml were centrifuged and the pelleted cells were resuspended in 1 l of M9 minimal medium, and grown at 37 °C until the OD was between 0.6 and 0.8. The cultures were cooled down to 20 °C, 0.3 g of solid pCMF were added (1.3 mM final concentration), and production of PCNA was induced with 1 mM IPTG and 0.02 % arabinose for 16 h at 20 °C. The cultures were grown in Erlenmeyer flasks 4-fold larger in volume than the culture volume and shaken at 200 rpm. Cells were harvested by centrifugation, resuspended in 6 ml of lysis buffer (20 mM Tris-HCl pH 7.6, 150 mM NaCl with protease inhibitors) per liter of culture and per OD unit, frozen in liquid nitrogen, and stored at −80 °C until purification. The cells were thawed, lysozyme (0.1 g/l) and DNAseI (1 mg/l) were added, the slurry was sonicated on ice and ultracentrifuged at 4 °C. The proteins were purified from the supernatant by four sequential chromatography steps. After filtration, the supernatant was injected in a 5 ml His-Trap column loaded with $Ni^{2+}$ ions and equilibrated in 20 mM Tris pH 7.6, 150 mM NaCl. After washing the column with buffer containing 25 mM imidazole, the protein was eluted with 500 mM imidazole in the same buffer. The total protein concentration in the PCNA containing fractions was estimated by absorbance at 280 nm and His-tagged HRV-3C protease was added (1:30 mass ratio) to cleave the affinity tag. Proteolysis proceeded during dialysis at 4 °C against buffer without imidazole for about 18 h. The mixture was loaded into the His-Trap column and the flowthrough diluted two-fold with 20 mM Tris-HCl pH 7.6 and injected in a 5 ml HiTrap Q HP column. PCNA was eluted with a linear gradient up to 1 M NaCl in 40 column volumes, pooled and injected into a preparative Superdex 200 column equilibrated in PBS (10 mM phosphate, 140 chloride, 153 sodium ion and 4.5 potassium ion) at pH 7.0 with 1 mM DTT. The fractions containing PCNA were pooled, concentrated to 3.4 g/l, frozen in liquid nitrogen and stored at −80 °C. All columns and

chromatography systems used were from Cytiva. Protein elution was monitored by absorbance at 280 nm and confirmed by SDS-PAGE. The purity and identity of the purified proteins were confirmed by Coomassie-stained SDS-PAGE, and MALDI-TOF mass spectrometry. The protein concentration was measured by absorbance at 280 nm using the extinction coefficient calculated from the amino acid composition corrected by removing the absorption of one tyrosine (as pCMF extinction coefficient is about 1.5 % of the one for Tyr at this wavelength). All indicated concentrations of PCNA samples refer to protomer concentrations. The purified protein contained the non-native sequence GPH at the N-terminus. The incorporation of pCMF instead of tyrosine in PCNA Y211-pCMF, was confirmed by trypsin digestion of the protein and analysis of the peptides by liquid chromatography electrospray ionization tandem mass spectrometry (LC/ESI-MS/MS).

The PIP peptides were purchased as lyophilized powders from Apeptide company. The 22-residue-long fragment of human p21 ($^{139}$GRKRR**Q**TS**M**TD**FY**HSKRRLIFS$^{160}$) and the 23-residue-long fragment of human p15 ($^{50}$GNPVCVRPTPKW**Q**KG**I**GE**FF**RLSPKDSE$^{77}$) are identical to the ones that have been co-crystalized with PCNA [6,8]. The 18-residue-long peptide YRRG$^{996}$TGKVGG**L**LA**F**AKRR$^{1009}$ corresponds to residues 996–1009 of the p125 subunit of human DNA-polymerase δ preceded by a non-native sequence to increase solubility (by increasing the net positive charge) and to measure accurately its concentration by light absorbance at 280 nm. The 28-residue-long peptide $^{458}$LHQETKPLPL**S**I**Q**N**S**L**D**L**FF**KEEELEYN$^{485}$ corresponds to residues 458–485 of human USP29. The residues in bold indicate those forming the PIP motif.

### 4.2. Size exclusion chromatography-multi angle light scattering (SEC-MALS)

The experiments were conducted at a temperature of 23 °C using a Superdex 200 Increase 10/300 GL column (Cytiva). The column was connected to a DAWN-EOS light scattering detector and an Optilab rEX differential refractive index detector from Wyatt Technology. Prior to the experiments, the column was equilibrated with PBS at pH 7.3 (filtered through a 0.1 μm membrane). A sample of 250 μl with PCNA Y211-pCMF protein at 1.5 g/l was injected into the system, and the chromatography was performed at a flow rate of 0.5 ml/min. Data acquisition and analysis were conducted using ASTRA software (Wyatt). To calibrate the SEC-MALS systems, a sample of Bovine Serum Albumin (BSA) at a concentration of 2 g/l in the same buffer was used. Through numerous measurements on BSA under similar conditions, we estimate that the experimental error in determining molar mass is approximately 5 %.

### 4.3. NMR spectroscopy

NMR spectra were recorded at 35 °C on a Bruker Avance III 800 MHz (18.8 T) spectrometer equipped with a cryogenically cooled triple resonance z-gradient probe. Samples with a volume of 400 μl of 60 or 50 μM U-[$^{2}$H,$^{13}$C, $^{15}$N] PCNA in PBS pH 7.0, 20 μM 2,2-dimethyl-2-silapentane-5-sulfonate, 0.01 % $NaN_3$, 1 mM DTT, and 5 % $^{2}H_2O$ were placed in a 5 mm Shigemi NMR tube (without plunger) and increasing volumes of peptide stocks at 3.9 (p125) or 3.8 (USP29) mM in PBS pH 7.0 were added and mixed by capping and inverting the NMR tube. BEST-$^{1}$H-$^{15}$N-TROSY spectra (p125 titration) were measured with 256 indirect points for 21 h. $^{1}$H-$^{15}$N HMQC spectra (USP29 titration) were measured with 128 indirect points for 11 h. The peptide-PCNA samples remained clear during the approximately 6 or 4 day-long titrations. The titrations allowed for an extensive transfer of backbone amide NMR signal assignments from the spectrum of free PCNA to the peptide-bound PCNA spectra, with a higher coverage in the TROSY than in the HMQC spectra because of their higher resolution. The CSP caused by the peptides were computed as the weighted average distance between the backbone amide $^{1}$H and $^{15}$N chemical shifts in the free and bound states [34]. The estimated error in the calculated CSP is ±0.005 ppm. The NMR spectrum of PCNA gives a single set of signals per residue, because it is a symmetric homotrimer. A single set of NMR signals along the titrations indicate that peptides bind identically to the three protomers in the PCNA ring without breaking its symmetry, as occurs with all PCNA-peptide complexes analyzed by NMR or calorimetry reported in the literature. The fitting of the CSP changes for those residues with CSP larger than the average plus two standard deviations was performed using a model of a single set of identical binding sites. The NMR-derived $K_D$ of the p125 peptide is the average over ten residues, with the standard deviation as an estimate of its uncertainty. The NMR-derived $K_D$ of the UP29 peptide is that of Gly127, with the fitting error as an estimate of its uncertainty.

### 4.4. Isothermal titration calorimetry

Measurements were performed using a MicroCal PEAQ-ITC calorimeter (Malvern) at 35 °*C*. Prior to measurements, protein and peptide stocks were dialyzed against PBS pH 7.0 with 1 mM TCEP against the same batch of buffer and degassed by ultrasonication for 5 min in a water bath. The sample cell was loaded with either PCNA at 10.1 μM (with p21_PIP) or 18.6 μM (with p15_PIP) or PCNA Y211-pCMF at 9.6 (with p21_PIP) or 18 μM (with p15_PIP) and the syringe with peptide stocks at concentrations 119, 346, 121, and 414 μM, respectively. The experimental setup involved a series of 19 injections, each consisting of 2 μl, with a time spacing of 150 s and a stirring speed of 750 rpm. The electrical power required to maintain a constant temperature in the reaction cell after each injection was recorded over time. The binding isotherms were fitted to a model corresponding to a single set of identical binding sites, taking into account heat dilution effects, using the MICROCAL PEAQ-ITC analysis software (Malvern). Each of the ITC measurements was done in duplicate or in triplicate, and the reported $K_D$ corresponds to the best fitting, with the fitting error as a measure of its uncertainty.

## CRediT authorship contribution statement

**Antonio Ruiz-Albor:** Writing – review & editing, Investigation. **Belén Chaves-Arquero:** Investigation. **Inés Martín-Barros:** Investigation. **Alejandra Guerra-Castellano:** Writing – review & editing, Methodology. **Amaia Gonzalez-Magaña:** Writing – review & editing, Investigation. **Alain Ibáñez de Opakua:** Writing – review & editing, Investigation. **Nekane Merino:** Methodology. **Mariola Ferreras-Gutiérrez:** Writing – review & editing, Methodology. **Edurne Berra:** Writing – review & editing, Project administration. **Irene Díaz-Moreno:** Writing – review & editing, Project administration. **Francisco J. Blanco:** Writing – review & editing, Writing – original draft, Project administration, Investigation, Funding acquisition, Conceptualization.

## Declaration of competing interest

The authors declare the following financial interests/personal relationships which may be considered as potential competing interests: Francisco J Blanco reports financial support provided by Spanish Ministry of Science and Innovation.

## Acknowledgements

We thank Tammo Diercks at CIC bioGUNE for help with NMR, Óscar Nuero and Carlos Alfonso at CIB-CSIC for help with SEC-MALS, and the Proteomics Unit at the Universidad Complutense de Madrid for the mass spectrometry analysis. This work was supported by the Agencia Estatal de Investigación (AEI), the Spanish Ministry of Science and Innovation (MCIN) and "ERDF A way of making Europe" (MCIN/AEI/10.13039/501100011033, grant numbers PID2020-113225GB-I00 to FJB, PID2021-126663NB-I00 to ID-M, and predoctoral contracts PRE2021-

099992 to ARA and PRE2018-085788 to MFG). Work at ID-M laboratory is also supported by The European Regional Development Fund (FEDER), the Andalusian Government (BIO-198), and the Ramón Areces Foundation. We also acknowledge the support from the network PIE-202120E047-Conexión-Life, CSIC.

## References

[1] S. Roa, E. Avdievich, J.U. Peled, T. Maccarthy, U. Werling, F.L. Kuang, R. Kan, C. Zhao, A. Bergman, P.E. Cohen, W. Edelmann, M.D. Scharff, Ubiquitylated PCNA plays a role in somatic hypermutation and class-switch recombination and is required for meiotic progression, Proc. Natl. Acad. Sci. U. S. A. 105 (42) (2008) 16248–16253.
[2] K.N. Choe, G.L. Moldovan, Forging ahead through darkness: PCNA, still the principal conductor at the replication fork, Mol. Cell 65 (3) (2017) 380–392.
[3] A. De Biasio, F.J. Blanco, Proliferating cell nuclear antigen structure and interactions: too many partners for one dancer? Adv. Protein Chem. Struct. Biol. 91 (2013) 1–36.
[4] A. Prestel, N. Wichmann, J.M. Martins, R. Marabini, N. Kassem, S.S. Broendum, M. Otterlei, O. Nielsen, M. Willemoes, M. Ploug, W. Boomsma, B.B. Kragelund, The PCNA interaction motifs revisited: thinking outside the PIP-box, Cell. Mol. Life Sci. 76 (24) (2019) 4923–4943.
[5] E.M. Boehm, M.T. Washington, R.I.P. to the PIP: PCNA-binding motif no longer considered specific: PIP motifs and other related sequences are not distinct entities and can bind multiple proteins involved in genome maintenance, Bioessays 38 (11) (2016) 1117–1122.
[6] J.M. Gulbis, Z. Kelman, J. Hurwitz, M. O'Donnell, J. Kuriyan, Structure of the C-terminal region of p21(WAF1/CIP1) complexed with human PCNA, Cell 87 (2) (1996) 297–306.
[7] M. De March, S. Barrera-Vilarmau, E. Crespan, E. Mentegari, N. Merino, A. Gonzalez-Magana, M. Romano-Moreno, G. Maga, R. Crehuet, S. Onesti, F. J. Blanco, A. De Biasio, p15PAF binding to PCNA modulates the DNA sliding surface, Nucleic Acids Res. 46 (18) (2018) 9816–9828.
[8] A. De Biasio, A.I. de Opakua, G.B. Mortuza, R. Molina, T.N. Cordeiro, F. Castillo, M. Villate, N. Merino, S. Delgado, D. Gil-Carton, I. Luque, T. Diercks, P. Bernado, G. Montoya, F.J. Blanco, Structure of p15(PAF)-PCNA complex and implications for clamp sliding during DNA replication and repair, Nat. Commun. 6 (2015) 6439.
[9] P.M.J. Burgers, T.A. Kunkel, Eukaryotic DNA replication fork, Annu. Rev. Biochem. 86 (2017) 417–438.
[10] J.B. Bruning, Y. Shamoo, Structural and thermodynamic analysis of human PCNA with peptides derived from DNA polymerase-delta p66 subunit and flap endonuclease-1, Structure 12 (12) (2004) 2209–2219.
[11] A. Gonzalez-Magana, A. Ibanez de Opakua, M. Romano-Moreno, J. Murciano-Calles, N. Merino, I. Luque, A.L. Rojas, S. Onesti, F.J. Blanco, A. De Biasio, The p12 subunit of human polymerase delta uses an atypical PIP box for molecular recognition of proliferating cell nuclear antigen (PCNA), J. Biol. Chem. 294 (11) (2019) 3947–3956.
[12] P. Khandagale, S. Thakur, N. Acharya, Identification of PCNA-interacting protein motifs in human DNA polymerase delta, Biosci. Rep. 40 (4) (2020).
[13] Y. Wang, Q. Zhang, H. Chen, X. Li, W. Mai, K. Chen, S. Zhang, E.Y. Lee, M.Y. Lee, Y. Zhou, P50, the small subunit of DNA polymerase delta, is required for mediation of the interaction of polymerase delta subassemblies with PCNA, PLoS One 6 (11) (2011) e27092.
[14] C. Lancey, M. Tehseen, V.S. Raducanu, F. Rashid, N. Merino, T.J. Ragan, C. G. Savva, M.S. Zaher, A. Shirbini, F.J. Blanco, S.M. Hamdan, A. De Biasio, Structure of the processive human Pol delta holoenzyme, Nat. Commun. 11 (1) (2020) 1109.
[15] F. Zheng, R.E. Georgescu, H. Li, M.E. O'Donnell, Structure of eukaryotic DNA polymerase delta bound to the PCNA clamp while encircling DNA, Proc. Natl. Acad. Sci. U. S. A. 117 (48) (2020) 30344–30353.
[16] N. Acharya, R. Klassen, R.E. Johnson, L. Prakash, S. Prakash, PCNA binding domains in all three subunits of yeast DNA polymerase delta modulate its function in DNA replication, Proc. Natl. Acad. Sci. U. S. A. 108 (44) (2011) 17927–17932.
[17] W. Leung, R.M. Baxley, G.L. Moldovan, A.K. Bielinsky, Mechanisms of DNA damage tolerance: post-translational regulation of PCNA, Genes (Basel) 10 (1) (2018).
[18] A. Mosbech, C. Lukas, S. Bekker-Jensen, N. Mailand, The deubiquitylating enzyme USP44 counteracts the DNA double-strand break response mediated by the RNF8 and RNF168 ubiquitin ligases, J. Biol. Chem. 288 (23) (2013) 16579–16587.
[19] S.C. Wang, Y. Nakajima, Y.L. Yu, W. Xia, C.T. Chen, C.C. Yang, E.W. McIntush, L. Y. Li, D.H. Hawke, R. Kobayashi, M.C. Hung, Tyrosine phosphorylation controls PCNA function through protein stability, Nat. Cell Biol. 8 (12) (2006) 1359–1368.
[20] J. Ortega, J.Y. Li, S. Lee, D. Tong, L. Gu, G.M. Li, Phosphorylation of PCNA by EGFR inhibits mismatch repair and promotes misincorporation during DNA synthesis, Proc. Natl. Acad. Sci. U. S. A. 112 (18) (2015) 5667–5672.
[21] Y.L. Wang, C.C. Lee, Y.C. Shen, P.L. Lin, W.R. Wu, Y.Z. Lin, W.C. Cheng, H. Chang, Y. Hung, Y.C. Cho, L.C. Liu, W.Y. Xia, J.H. Ji, J.A. Liang, S.F. Chiang, C.G. Liu, J. Yao, M.C. Hung, S.C. Wang, Evading immune surveillance via tyrosine phosphorylation of nuclear PCNA, Cell Rep. 36 (8) (2021) 109537.
[22] J. Xie, L. Supekova, P.G. Schultz, A genetically encoded metabolically stable analogue of phosphotyrosine in Escherichia coli, ACS Chem. Biol. 2 (7) (2007) 474–478.
[23] M. Hedglin, B. Pandey, S.J. Benkovic, Stability of the human polymerase delta holoenzyme and its implications in lagging strand DNA synthesis, Proc. Natl. Acad. Sci. U. S. A. 113 (13) (2016) E1777–E1786.
[24] C. Lancey, M. Tehseen, S. Bakshi, M. Percival, M. Takahashi, M.A. Sobhy, V. S. Raducanu, K. Blair, F.W. Muskett, T.J. Ragan, R. Crehuet, S.M. Hamdan, A. De Biasio, Cryo-EM structure of human Pol kappa bound to DNA and mono-ubiquitylated PCNA, Nat. Commun. 12 (1) (2021) 6095.
[25] K. Blair, M. Tehseen, V.S. Raducanu, T. Shahid, C. Lancey, F. Rashid, R. Crehuet, S. M. Hamdan, A. De Biasio, Mechanism of human Lig1 regulation by PCNA in Okazaki fragment sealing, Nat. Commun. 13 (1) (2022) 7833.
[26] S.M. Hamdan, A. De Biasio, Functional hierarchy of PCNA-interacting motifs in DNA processing enzymes, Bioessays 45 (6) (2023) e2300020.
[27] M.J. Clague, I. Barsukov, J.M. Coulson, H. Liu, D.J. Rigden, S. Urbe, Deubiquitylases from genes to organism, Physiol. Rev. 93 (3) (2013) 1289–1315.
[28] A. Hendel, P.H. Krijger, N. Diamant, Z. Goren, P. Langerak, J. Kim, T. Reissner, K. Y. Lee, N.E. Geacintov, T. Carell, K. Myung, S. Tateishi, A. D'Andrea, H. Jacobs, Z. Livneh, PCNA ubiquitination is important, but not essential for translesion DNA synthesis in mammalian cells, PLoS Genet. 7 (9) (2011) e1002262.
[29] M. Hedglin, B. Pandey, S.J. Benkovic, Characterization of human translesion DNA synthesis across a UV-induced DNA lesion, Elife 5 (2016).
[30] O. Cazzalini, S. Sommatis, M. Tillhon, I. Dutto, A. Bachi, A. Rapp, T. Nardo, A. I. Scovassi, D. Necchi, M.C. Cardoso, L.A. Stivala, E. Prosperi, CBP and p300 acetylate PCNA to link its degradation with nucleotide excision repair synthesis, Nucleic Acids Res. 42 (13) (2014) 8433–8448.
[31] P. Billon, J. Cote, Novel mechanism of PCNA control through acetylation of its sliding surface, Mol. Cell. Oncol. 4 (2) (2017) e1279724.
[32] T.S. Young, I. Ahmad, J.A. Yin, P.G. Schultz, An enhanced system for unnatural amino acid mutagenesis in E. coli, J. Mol. Biol. 395 (2) (2010) 361–374.
[33] A. Guerra-Castellano, A. Diaz-Quintana, B. Moreno-Beltran, J. Lopez-Prados, P. M. Nieto, W. Meister, J. Staffa, M. Teixeira, P. Hildebrandt, M.A. De la Rosa, I. Diaz-Moreno, Mimicking tyrosine phosphorylation in human cytochrome c by the evolved tRNA synthetase technique, Chemistry 21 (42) (2015) 15004–15012.
[34] A. De Biasio, R. Campos-Olivas, R. Sanchez, J.P. Lopez-Alonso, D. Pantoja-Uceda, N. Merino, M. Villate, J.M. Martin-Garcia, F. Castillo, I. Luque, F.J. Blanco, Proliferating cell nuclear antigen (PCNA) interactions in solution studied by NMR, PLoS One 7 (11) (2012) e48390.